

High-spin structures of $^{86,87,88,89}\text{Y}$: a shell model interpretation

P. C. Srivastava^{1 a}, Vikas Kumar¹ and M. J. Ermamatov²

¹ Department of Physics, Indian Institute of Technology, Roorkee 247 667, India

² Institute of Nuclear Physics, Ulughbek, Tashkent 100214, Uzbekistan

October 11, 2018

Abstract. In this work nuclear structure properties of $^{86,87,88,89}\text{Y}$ isotopes have been investigated using large-scale shell-model calculations within the full $f_{5/2}pg_{9/2}$ model space. The calculations have been performed with JUN45 and jj44b effective interactions that have been proposed for use in the $f_{5/2}$, $p_{3/2}$, $p_{1/2}$, $g_{9/2}$ model space for both protons and neutrons. Reasonable agreement between experimental and calculated values are obtained. This work will add more information to previous study by projected shell model [Eur. Phys. J. A 48, 138 (2012)] where full-fledged shell model calculations proposed for these nuclei.

PACS. 21.60.Cs Shell model

1 Introduction

The neutron rich nuclei with $Z = 28-40$ recently attracted much theoretical and experimental affords [1, 2, 3, 4, 5, 6, 7, 8, 9, 10]. Many fascinating phenomena have been observed in this region. The nuclei Sr, Y and Zr are close to subshell closure, thus they are expected to exhibit single-particle characteristics. The other important features in this region are existence of high-spin isomers and shape transitions as higher j orbitals are occupied. Recently structure of Sr and Zr isotopes near and at the magic number $N = 50$ shell via g -factor and life-time measurements have been investigated. The Zr isotopes changing structure from ^{80}Zr (super deformed) with high occupancy of $\pi g_{9/2}$ orbit to less deformed ^{90}Zr with substantial $\pi g_{9/2}$ orbit occupancy. Recent experimental study claim the evolution of collectivity and shape coexistence for Sr isotopes.

The high-spin states in ^{86}Y using heavy-ion fusion-evaporation reactions have been studied in [11]. The corresponding structures were interpreted by shell-model with truncation. For ^{88}Y the high-spin states up to an excitation energy of 8.6 MeV and spin and parity of $19^{(-)}$ reported in Ref. [12]. In the another experiment high-spin states up to spin $21\hbar$ investigated through fusion-evaporation reaction $^{82}\text{Se} (^{11}\text{B}, 5n)$ [13]. The excited states of ^{87}Y up to $33/2^{(-)}$ at ~ 7 MeV with in-beam γ ray spectroscopy reported in [14]. In this work majority of the observed high-spin states explain on the basis of $\nu = 3$ and $\nu = 5$ configurations. Previously this nucleus were experimentally studied in Refs. [15, 16, 17], and excited states up to ~ 4.6 MeV were observed. The experimental results up to $31/2^+$ \hbar for ^{89}Y is reported in [18] by using in-beam γ -ray spectroscopy. B. Cheal *et al.* used laser

spectroscopy method to study isomeric states of yttrium isotopes [19]. In this work nuclear charge radii differences, magnetic dipole and electric quadrupole moments have been obtained. Recently, theoretical results of positive - parity yrast bands of odd $^{79-89}\text{Y}$ isotopes using projected shell model (PSM) reported in [20]. In this work it is mentioned that the results of large-scale shell model calculation in this mass region is limited due to involvement of $g_{9/2}$ orbital which generate large configuration space. Thus results of modern shell-model calculations are desire for these nuclei.

In the present paper, we reported systematic study of shell-model results for $^{86,87,88,89}\text{Y}$ isotopes. The main motivation of present study to explain recently available experimental data for these isotopes.

The result of present work is organized as follows: Model space and Hamiltonian is given in section 2. In section 3-5, energy levels and transition probabilities, quadrupole and magnetic moments, occupancy are compared with the available experimental data. Finally, concluding remarks are drawn in section 6.

2 Model space and Hamiltonians

The present shell model (SM) calculations have been carried out with two recently available effective SM interactions, JUN45 and jj44b, that have been proposed for the $1p_{3/2}$, $0f_{5/2}$, $1p_{1/2}$ and $0g_{9/2}$ single-particle orbits. JUN45, which was recently developed by Honma *et al* [21], is a realistic interaction based on the Bonn-C potential fitting 400 experimental binding and excitation energy data with mass numbers $A = 63-96$. Since the present model space is not sufficient to describe collectivity in these regions, data have not been used while fitting in the middle of the

^a e-mail: pcsrifph@iitr.ac.in

shell along the $N = Z$ line. For JUN45, the data mostly fitted to develop this interaction closure to $N = 50$. This interaction is not successful in explaining data for Ni and Cu isotopes, possibly due to the missing $0f_{7/2}$ orbit in the present model space. The jj44b interaction due to Brown et al [22] was developed by fitting 600 binding energies and excitation energies with $Z = 28-30$ and $N = 48-50$. Instead of 45 as in JUN45, here 30 linear combinations of good JT two-body matrix elements (TBME) varied, with the rms deviation of about 250 keV from experiment. For the JUN45 interaction, the single-particle energies are taken to be -9.8280, -8.7087, -7.8388 and -6.2617 MeV for the $p_{3/2}$, $f_{5/2}$, $p_{1/2}$ and $g_{9/2}$ orbits, respectively. Similarly for the jj44b interaction, the single-particle energies are taken to be -9.6566, -9.2859, -8.2695 and -5.8944 MeV for the $p_{3/2}$, $f_{5/2}$, $p_{1/2}$ and $g_{9/2}$ orbits, respectively.

All calculations in the present paper are carried out at TLAPOA computational facility at ICN, UNAM, Mexico using the shell model code ANTOINE.[23] In case of ^{79}Se for positive parity maximal dimension is 59 791822.

3 Result of Y isotopes

The shell model results for $^{86-89}\text{Y}$ with two different interactions are shown in Figs. 1–4.

3.1 ^{86}Y

Previously shell model calculation in $f_{5/2}pg_{9/2}$ space for this isotope with truncation by allowing up to two particles excitation from $f_{5/2}$ and $p_{3/2}$ to $p_{1/2}$ and $g_{9/2}$ is reported in Ref. [11]. The signature splitting and magnetic rotation of ^{86}Y using self-consistent tilted axis cranking calculations based on relativistic mean field theory to investigate the dipole structures have been studied by Li *et al* [24]. In present study we performed shell model calculation in $f_{5/2}pg_{9/2}$ space, this will add more information in the previous study [11] where truncated shell model results reported.

The JUN45 predicts the same sequence of the first four levels as in the experiment, however 7^- level is much higher than in the experiment. This level is better predicted by jj44b, but the other two levels are lower than in the experiment. All the calculated levels up to 17^- have lower values in both calculations than in the experiment. Then the value of 18^- comes very close to the experimental one. The 19^- is little bit lower in JUN45 calculation and in jj44b the calculated value of this level becomes ~ 300 keV larger as compared to experimental one.

The 8^+ level at 218 keV predicted to be 181 and 74 keV by JUN45 and jj44b calculations, respectively. Then sequence of two 1^+ levels are the same in jj44b calculation. The value of the first 1^+ level in this calculation is lower than in the experiment and that of second level is higher. In JUN45 both levels are located higher than in the experiment. A very good agreement is given by both calculation starting from 9^+ until 15^+ . Then both calculations starts to differ from the experiment. For the ground state 4^- ,

the JUN45 interaction predicting $\pi(p_{1/2}^1) \otimes \nu(g_{9/2}^{-3})$ ($\sim 30\%$) configuration while jj44b as $\pi(g_{9/2}^3) \otimes \nu(f_{5/2}^{-1})$ ($\sim 17\%$).

3.2 ^{87}Y

Both calculations predict correct ground state. In the jj44b calculation the sequence of next four negative parity levels are the same as in the experiment, though the values of this levels are lower than the experimental ones. The $13/2^-$ level is lower than in the experiment while $11/2^-$ is higher than in the experiment, but the difference in $15/2^-$ experimental and calculated values is only 3 keV. The $23/2^-$ levels which appear in the calculation have not been measured in the experiment. Then the values of next $25/2^-$ levels are ~ 300 keV lower than in the experiment. Last four $27/2^-$, $29/2^-$, $31/2^-$ and $33/2^-$ levels are in good agreement with the experimental data.

In JUN45 calculation the pair of $3/2^-$, $5/2^-$ and $1/2^-$, $9/2^-$ levels are interchanged as compared to the experiment. The $1/2^-$ level is much closer to the experiment than in jj44b calculation.

Positive parity levels start from $9/2^+$ in the experiment and in both calculations. In jj44b it starts from lower value than in the experiment. The $7/2^+$ level appearing in both calculations has not been measured in the experiment. Then $5/2^+$ and $13/2^+$ levels are lower than in the experiment in jj44b calculation while they are higher in the JUN45 calculation. Better agreement with the experiment in higher spins gives JUN45 calculation. The structure of ground state $1/2^-$ is a single-particle character ($\pi(p_{1/2}^1)$). The JUN45 and jj44b interactions predicting $\sim 41\%$ and $\sim 22\%$ probability, respectively.

3.3 ^{88}Y

The first three negative parity levels are in better agreement with the experiment in JUN45 calculation, while the values of these levels are smaller in the jj44b calculation. The 7^- , 8^- and 9^- levels which appear in both calculation have not been measured in the experiment. Then the levels up to the 15^- are better predicted by JUN45 calculation. The other calculated higher spin levels have larger values than in the experiment.

The sequence of the first two positive parity levels is the same as in the experiment in JUN45 calculation and the values of these levels are higher than in the experiment. In the jj44b calculation these levels are predicted lower and 7^+ and 8^+ levels are interchanged with respect to the experimental ones. The 9^+ levels is located higher in JUN45, while it is lower in jj44b calculation. The value closer to the experimental one is predicted by JUN45 calculation for 10^+ level. The 10^+ , 11^+ , 12^+ and 13^+ levels which appear in the calculation have not been measured in the experiment. The levels predicted by JUN45 from 16^+ to 18^+ have larger values as compared to experimental ones, while 16^+ and 17^+ have smaller values than in

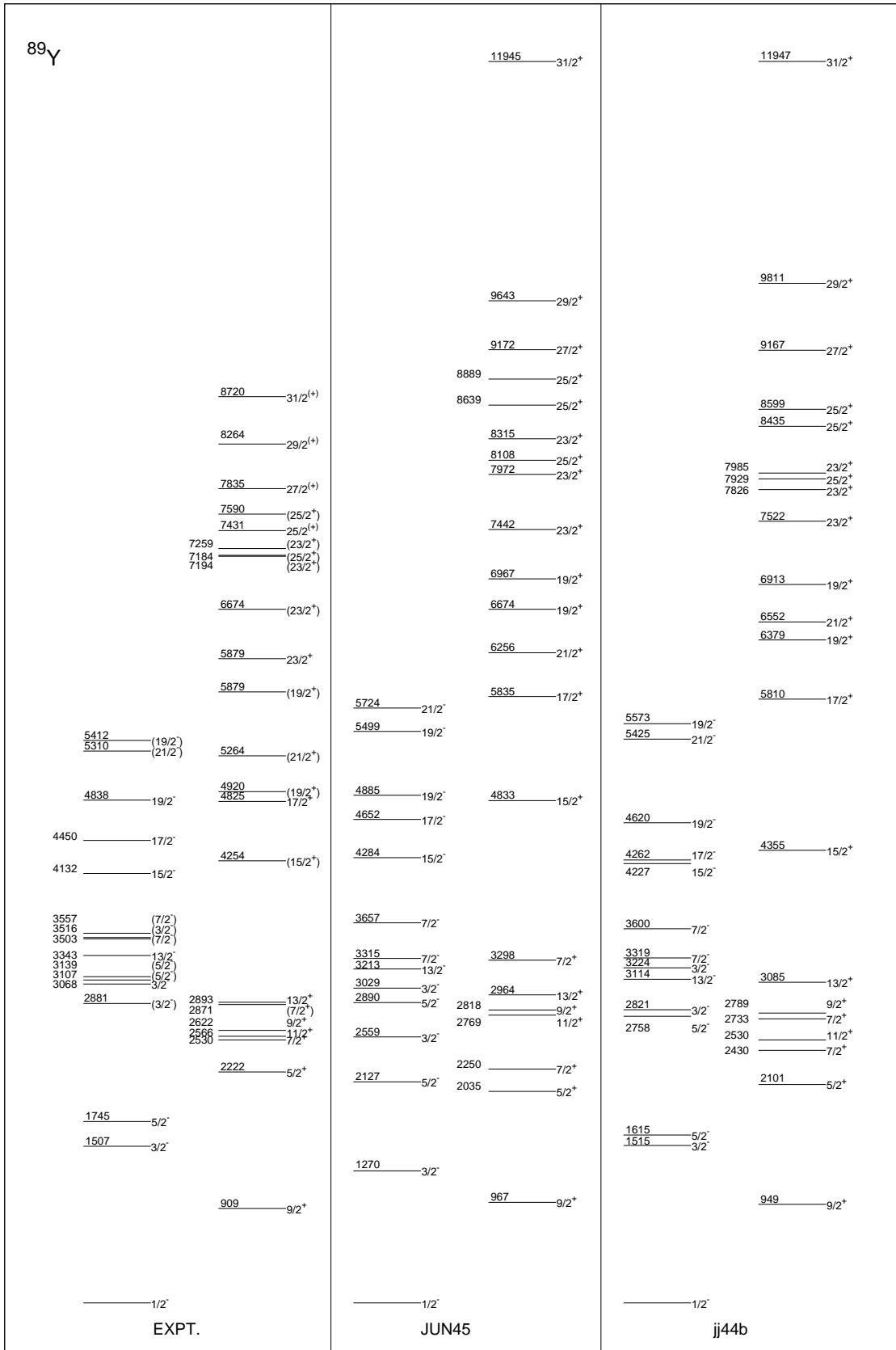


Fig. 4. Comparison of shell-model results with experimental data for ^{89}Y with different interactions.

Table 1. $B(E2)$ reduced transition strength in W.u. Experimental values were taken from the NNDC database.

	$I_i^{\pi} \rightarrow I_f^{\pi}$	E_{γ}	Exp.	JUN45	jj44b
^{86}Y	$4^{-} \rightarrow 2^{-}$	242.80	1.00 (8)	2.12	0.08
	$(8^{+}) \rightarrow (10^{+})$	1107.08	> 0.030	11.67	18.06
	$(10^{+}) \rightarrow (12^{+})$	1195.88	> 0.021	10.74	22.04
^{88}Y	$(8^{+}) \rightarrow (10^{+})$	1769.35	> 0.6233	9.30	9.34
	$(10^{+}) \rightarrow (12^{+})$	1195.88	> 0.021	5.44	0.91
^{87}Y	$1/2^{-} \rightarrow 5/2^{-}$	793.7	≥ 0.0078	6.54	1.06
	$13/2^{+} \rightarrow 17/2^{+}$	1023.6	≥ 0.0022	7.53	18.30
	$17/2^{+} \rightarrow 21/2^{+}$	399	4.6 (3)	3.99	5.00
	$21/2^{+} \rightarrow (23/2^{+})$	159.8	≥ 4.1	7.51	9.90
	$21/2^{+} \rightarrow (25/2^{+})$	1782.4	4.9 (21)	5.67	6.76
	$9/2^{+} \rightarrow 5/2^{+}$	1313.2	4.3 (13)	2.99	3.22
^{89}Y	$9/2^{+} \rightarrow 13/2^{+}$	1984.1	4.3(8)	7.98	8.50
	$13/2^{+} \rightarrow 17/2^{+}$	1931.9	< 0.029	0.98	6.69
	$21/2^{+} \rightarrow (25/2^{+})$	1920.2	4.4(18)	5.94	3.26
	$25/2^{(+)} \rightarrow (29/2^{+})$	832.9	< 8	0.53	5.84
	$27/2^{(+)} \rightarrow (31/2^{+})$	885.9	< 19	1.09	0.02
	$1/2^{-} \rightarrow 5/2^{-}$	1744.7	2.3	5.38	5.29
	$13/2^{-} \rightarrow 17/2^{-}$	1106.5	2.1(5)	2.24	0.12
	$15/2^{-} \rightarrow 19/2^{-}$	706.3	2.2(10)	1.55	3.09
	$17/2^{-} \rightarrow (21/2^{-})$	860.1	0.57(15)	0.93	2.27

the experiment in jj44b calculation. The 19^{+} level in both calculations is close to the experimental level at 9142 keV, to which in the experiment spin has yet not been assigned. Both interactions predicting $\pi(p_{1/2}^1) \otimes \nu(g_{9/2}^{-1})$ configuration for ground state 4^{-} with probability $\sim 57\%$ (JUN45) and $\sim 46\%$ (jj44b).

3.4 ^{89}Y

Both calculations predict $1/2^{-}$ ground state as in the experiment. In the JUN45 calculation the spacing between $3/2^{-}$ and $5/2^{-}$ levels are much higher than in the experiment. In the jj44b calculation these two levels are closer to the experiment and little bit compressed as compared to the experiment. The $3/2_1^{-}$ and $3/2_2^{-}$ predicted better by jj44b calculation. The $5/2_2^{-}$ level in the experiment predicted lower by JUN45 and even more lower by jj44b. Both calculations gives small difference in the sequence of the next experimental $13/2^{-}$, $(7/2)^{-}$, $(3/2)^{-}$ and $(7/2)^{-}$ levels, though the location of $3/2^{-}$ level looks better in jj44b calculation. The sequence of last five experimental levels are exactly the same as in the experiment in jj44b calculation and the values of these levels are closer to the experimental ones than in JUN45 calculation.

Agreement of positive parity levels with the experimental ones become much improved in both calculation for the ^{89}Y as compared to ^{87}Y until $15/2^{+}$. Then both calculations predict higher values than in the experiment. As we move from ^{87}Y to ^{89}Y the ground state $1/2^{-}$ is the same with configuration i.e. $\pi(p_{1/2}^1)$, now probability become $\sim 71\%$ (JUN45) and $\sim 67\%$ (jj44b).

Table 2. Electric quadrupole moments, Q_s (in eb), the effective charges $e_p=1.5 e$, $e_n=0.5 e$ are used in the calculation and magnetic moments, μ (in μ_N), for $g_s^{eff} = 0.7g_s^{free}$.

	^{86}Y	^{88}Y	^{87}Y	^{89}Y
	$Q(8_1^+)$	$Q(8_1^+)$	$Q(9/2_1^+)$	$Q(9/2_1^+)$
Experiment	+N/A	+0.06(6)	-0.50(6)	-0.43(6)
JUN45	-0.16	-0.022	-0.44	-0.27
jj44b	-0.03	+0.005	-0.48	-0.34
			$\mu(9/2_1^+)$	$\mu(9/2_1^+)$
Experiment			+6.24(2)	+6.37(4)
JUN45			+6.59	+6.81
jj44b			+6.42	+6.56

4 Reduced transition probability, quadrupole and magnetic moments

The electric multipoles of order L are defined as

$$B(eL, L) = \frac{1}{2J_i + 1} | \langle J_f || \sum_i e_i r_i^L Y_L(\theta_i, \phi_i) || J_i \rangle |^2, \quad (1)$$

where J_i and J_f are the initial and final state spins, respectively.

The $B(E2)$ values is defined as

$$B(E2) = \frac{1}{2J_i + 1} | \langle J_f || \sum_i e_i r_i^2 Y_2(\theta_i, \phi_i) || J_i \rangle |^2. \quad (2)$$

The experimentally determined $B(E2)$ values, for different transitions is listed in table 1. In this table we have also listed value of E_{γ} for corresponding transitions. The theoretical calculations were performed employing effective charges: $e_{\text{eff}}^{\pi} = 1.5 e$, $e_{\text{eff}}^{\nu} = 0.5 e$ for two set of effective interactions. The overall results for JUN45 interaction show better agreement with experimental data.

In table 2, we have also compare quadrupole and magnetic moments with available experimental data. The results are close to experimental data. Thus we may conclude that the present model space is sufficient to predict this property. There is no need to include proton $f_{7/2}$ orbital in the model space to see the importance of the proton excitation across $Z = 28$ shell.

5 Occupancy

We have plotted occupancy of proton/neutron orbitals for $^{86,87,88,89}\text{Y}$ in Fig. 5. As we move from ^{86}Y to ^{89}Y the proton occupancy for $f_{5/2}$ orbital is increasing while the occupancy of $g_{9/2}$ orbital is decreasing. While in the case of the neutrons, the occupancy of both $f_{5/2}$ and $g_{9/2}$ orbitals is increasing. This reflects that as we move towards ^{89}Y ,

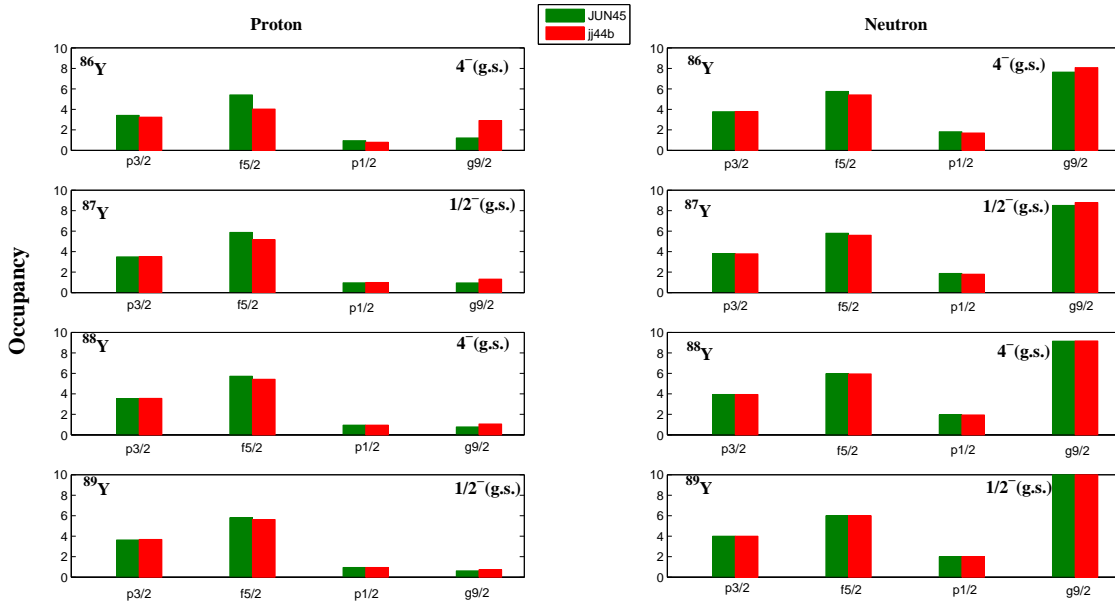


Fig. 5. Occupancy of proton/neutron orbitals for ground state in $^{86,87,88,89}\text{Y}$ isotopes.

the neutrons prefer to occupy $g_{9/2}$ orbital. The occupancy of neutron $p_{1/2}$ orbital is greater than proton $p_{1/2}$ orbital and it is continuously increasing in the case of jj44b interaction. The $p_{3/2}$ orbital occupancy is always increasing for both interactions as we move towards ^{89}Y .

6 Conclusions

In the present work we performed full-fledged shell model calculation for $^{86,87,88,89}\text{Y}$ isotopes in $f_{5/2}p_{3/2}g_{9/2}$ model space. Following conclusions have been drawn from this work:

- The calculated energy levels, $B(E2)$'s, quadrupole and magnetic moments are in good agreement with experimental data.
- Further theoretical development for identification of intruder orbitals including $d_{5/2}$ orbital in the model space is needed to study excitation across $N = 50$ shell for better identification of the structure of these nuclei.
- Both interactions predicting $\pi(p_{1/2}^1)$ configuration for ground state ($1/2^-$) for $^{87,89}\text{Y}$, while in case of ^{88}Y ground state (4^-) has $\pi(p_{1/2}^1) \otimes \nu(g_{9/2}^{-1})$ configuration.
- For the ground state the neutron occupancy is increasing for $f_{5/2}$ and $g_{9/2}$ orbitals as we move from ^{86}Y to ^{89}Y .

Acknowledgment

All the shell-model calculations have been carried out at TLAPOA computational facility at ICN, UNAM, Mexico. This work is supported by CSIR fellowship of India. MJE

acknowledges support from the grant No. F2-FA-F177 of Uzbekistan Academy of Sciences.

References

1. G. Hagen, M. Hjorth-Jensen, G. R. Jansen, R. Machleidt, and T. Papenbrock, Phys. Rev. Lett. **109**, 032502 (2012).
2. K. Kaneko, T. Mizusaki, Y. Sun, and S. Tazaki, Phys. Rev. C **89**, 011302(R) (2014).
3. O. Sorlin and M.-G. Porquet, Phys. Scr. T**152**, 014003 (2013).
4. J. D. Holt, T. Otsuka, A. Schwenk and T. Suzuki, J. Phys. G **39**, 085111 (2012).
5. S.M. Lenzi, F. Nowacki, A. Poves, and K. Sieja, Phys. Rev. C **82**, 054301 (2010).
6. D. Steppenbeck *et al.*, Phys. Rev. C **85**, 044316 (2012).
7. S. L. Rice *et al.*, Phys. Rev. C **88**, 044334 (2013).
8. P.C. Srivastava and I. Mehrotra, Eur. Phys. J A **45**, 185 (2010).
9. P.C. Srivastava, J. Phys. G **39**, 015102 (2012).
10. P.C. Srivastava, M.J. Ermamatov and I.O. Morales, J. Phys. G **40**, 035106 (2013).
11. C. Rusu *et al.*, Nucl. Phys. A **818**, 1 (2009).
12. M. Bunce *et al.*, Phys. Rev. C **87**, 044337 (2013).
13. C.J. Xu *et al.*, Phys. Rev. C **86**, 027302 (2012).
14. R. Schwenger *et al.*, Phys. Rev. C **57**, 2892 (1998).
15. I. C. Oelrich *et al.*, Phys. Rev. C **14**, 563 (1976).
16. C.A. Fields *et al.*, Z. Phys. A **295**, 365 (1980).
17. E.K. Warburton *et al.*, J. Phys. G **12**, 1017 (1986).
18. L. Funke *et al.*, Nucl. Phys. A **541**, 241 (1992).
19. B. Cheal *et al.*, Phys. Lett. B **645**, 133 (2007).
20. C. Sharma *et al.*, Eur. Phys. J A **48**, 138 (2012).
21. M. Honma *et al.*, 2009 Phys. Rev. C **80** 064323 (2009).
22. B.A. Brown and A.F. Lisetskiy (unpublished).
23. E. Caurier, G. Martínez-Pinedo, F. Nowacki, A. Poves, and A. P. Zuker Rev. Mod. Phys. **77** 427 (2005).
24. J. Li, Phys. Rev. C **88** 014317 (2013).